Proceedings of the
44th IEEE Conference on Decision and Control, and
the European Control Conference 2005
Seville, Spain, December 12-15, 2005

Active Control of Flow Over a Backward-Facing Step

Abbas Emami-Naeini, Sarah A. McCabe, Dick de Roover, Jon L. Ebert, Robert L. Kosut

Abstract—**We describe a control-oriented model reduction process from partial differential equation (PDE) descriptions of aerodynamic flow systems, and the design of low-order feedback controllers using these procedures. An effective approach for flow model reduction for active control using balanced truncation approaches was developed. The techniques were applied to a flow control problem representative of aerospace problems: active control of flow over a modified 2D backward-facing step, which can be handled by most commercial finite element packages. Although the geometry is rather simple, the richness of the flow field is well documented. Feedback controllers were developed for disturbance rejection and tracking of the reattachment point for both high and low Reynolds numbers.**

I. Introduction

During the past two decades, there has been substantial effort to develop methodologies and tools to actively control fluid flow phenomena [1]-[4]. Possible applications include separation control, drag reduction, lift enhancement, and virtual aerodynamic shaping. The effort has consisted of analytical approaches, numerical simulations, and experimental work. The focus on active control of fluid dynamics has resulted in application of control-theoretic approaches to nonlinear partial differential equations (PDEs), and development of low-order physical models for control design. The development of physics-based low-dimensional models is a promising avenue toward active flow control [6]-[10], [15].

In this paper, we describe feedback control design of active flow control based on reduced order models from balanced truncation and system identification. The method was applied to a problem that is representative of aerospace applications: flow over a modified 2D backward-facing step [11]-[14]. Nonlinear models were developed for both high and low Reynolds numbers that are three orders of magnitude apart. Feedback control designs were carried out for both disturbance rejection and tracking of the commanded reattachment point location for both high and low Reynolds number cases. The feasibility of the methods was demonstrated by linear and nonlinear simulations. For the characteristics of the flow we considered a plant model of order only *four* is sufficient to capture the control relevant dynamics.

Manuscript received March 4, 2005. This work was supported in part by AFOSR under Contract F49620-03-C-0112. The program monitor was Lt. Col. Sharon Heise, USAF, Ph.D.

The authors are with SC Solutions, Inc., Systems & Control Division, 1261 Oakmead Pkwy, Sunnyvale, CA 94085 USA (e-mail: emami@scsolutions.com).

II. Case Study: Flow over a Backward-facing Step

Separation and reattachment flow occurs in many aerospace related systems such as diffusers, combustors, etc. Among the flow geometries used to study separated flows, the backward-facing step is common [13]-[14]. The flow over a backward-facing step has a simple geometry and also has flow characteristics similar to fully stalled diffuser flow [11]-[12]. Even though the geometry is simple, the flow involves complicated streamlines as shown in Figure 1 [11]. The separation is fixed by a sharp corner as shown. Therefore, the separation-reattachment process can be examined by itself. The boundary layer separates at the edge of the step, and a free-shear layer develops inside the original shear layer. Part of the flow is reversed toward the step and re-entrained into the shear layer in the reattachment zone, which results in the formation of a recirculating zone behind the step. A new boundary layer grows on the surface downstream of the reattachment point. This layer then interacts with the approaching shear layer that flows over it from upstream. The separation-reattachment process is thus characterized by a complex interaction between the separated shear layer and the adjacent flow [11]-[14]. The location of the reattachment point is a good indicator of the dynamic flow behavior, and control of the location of this point can be used to control overall flow characteristics. In this paper, we discuss active control of the location of this point by suction and blowing.

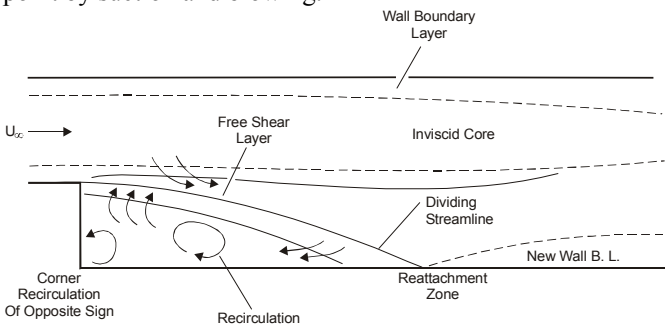

Figure 1. Schematic of streamlines in separation-reattachment process [12].

A specific flow example (illustrated in Figure 2) was used to demonstrate model reduction for separation control. This is the classical example of turbulent flow over a backward-facing step with a modification representative of boundary flow control in an aerospace system. In this example, a flow with mean velocity v enters the channel from the left and passes over a backward-facing step. Optional suction or blowing control, u, on the step face allows control of

0-7803-9568-9/05/$20.00 ©2005 IEEE

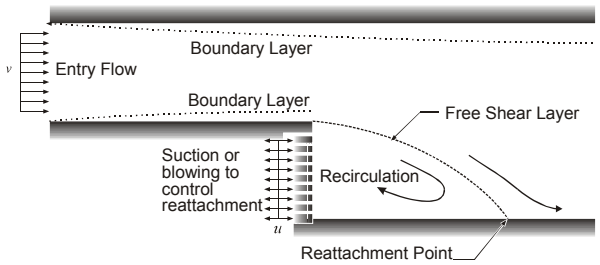

Figure 2. Turbulent flow over a backward-facing step with controls.

important aspects of the flow, e.g., the location of the reattachment point. The addition of blowing or suction on the step face allows control of the position where the flow reattaches. If fluid is injected on the step (blowing $u > 0$) the reattachment will move downstream, while suction ($u < 0$) will draw it upstream. The relation between flow/velocity sensor locations and flow control power (under feedback) can be studied with this model. In addition, by varying the entry flow velocity, v, the model can be used to study control of transient flow. The specific benchmark example (with dimensions and parameters) is shown in Figure 3.

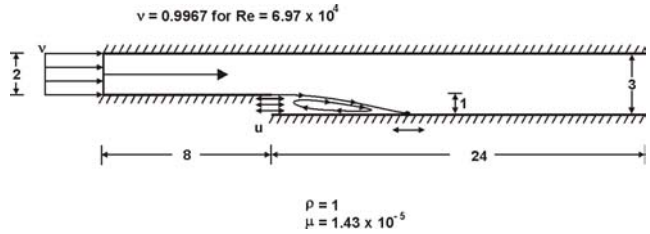

Figure 3. Benchmark flow control problem: 2D backward-facing step.

This example will illustrate separation control for the 2D case. The idea is to control the location of the reattachment point on the lower wall using (distributed) measurements of velocity (from micro-electro-mechanical (MEMS) sensors) along the lower wall. The actuator is the suction/blowing, u. The dimensions shown are in meters and the velocity is in units of m/s, the kinematic viscosity, μ, has units of kg/(m.s), and the density, ρ, has units of kg/m^3.

In this paper we consider both a disturbance rejection as well as a tracking control problem. The control problem is defined as follows. Assume the nominal value of v = 1m/sec and u ranges between ± 0.1m/sec. We run the Navier-Stokes simulation to steady-state to establish the streamlines and determine the location of the (nominal) reattachment point on the lower wall. For disturbance rejection, we introduce a constant disturbance onto v so that $v = 1 + d$. We use feedback from the measurement of the reattachment point, y, to the control, u, to move the reattachment point back to its original position. For tracking the reattachment point, we let $d = 0$. We command the reattachment point as desired to fore/aft of the nominal reattachment point. We wish to move the reattachment point up or down and hold it at a desired position. We will now address the nonlinear and linear model generation for the backward-facing step case study.

III. Nonlinear Model for Flow over a Backward-facing Step

Nonlinear models were developed using the commercial software ADINA® for both high and low Reynolds numbers that are three orders of magnitude apart. ADINA® is a general purpose finite element commercial software package for linear and nonlinear analysis of structural, heat transfer, field and fluid flow problems. ADINA® is an unsteady Reynolds averaged Navier Stokes (RANS) solver. For the high Reynolds number case we used Re = 6.97×10^4. A set of finite element models of the system was constructed. The steady-state solution for the nominal operating point of this system (u = 0, v = 1.0) was obtained using an 881-node mesh constructed in a non-uniform manner so as to increase the model accuracy in the regions of primary interest. Mesh refinements were carried out to obtain a converged solution. In particular, ADINA® simulation runs were performed for N = 881 nodes, ~2N, ~3N, ~4N, ~5N, ~7N, ~8N, ~9N, ~10N, ~11N, and ~15N. The sample result for the flow field for ~11N is shown in Figure 4. The corresponding velocity vectors of the solution with zooming in on the vicinity of the step are shown in Figure 5. It is evident from our results that for the high- fidelity solutions (~11N, ~15N) a second recirculation zone has formed at the corner of the

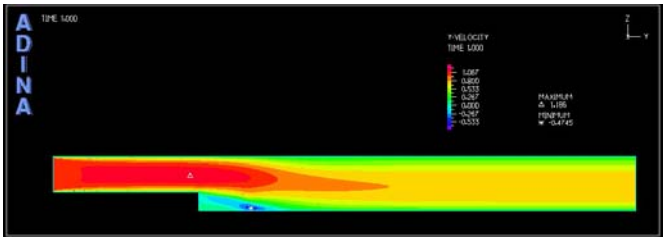

Figure 4. Flow field for 9433 nodes (~11N) with reattachment point = 4.58m (for Re = 6.97×10^4).

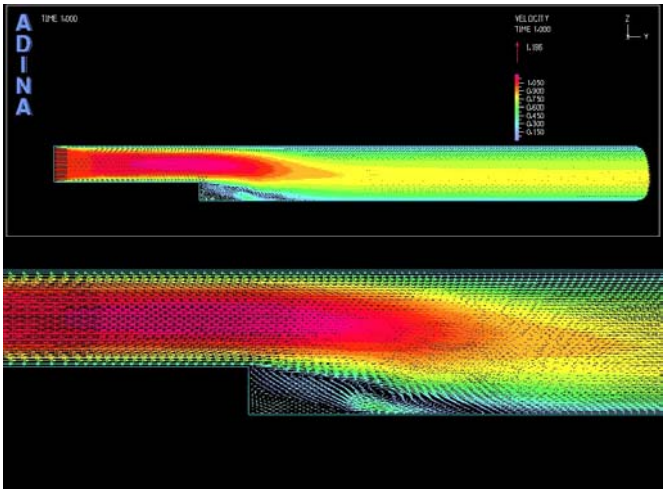

Figure 5. Velocity vectors for 9433 nodes (~11N) with reattachment point = 4.58m (for Re = 6.97×10^4).

step as shown in Figure 5. The velocity profiles were computed for various y distances. By comparing velocity profiles with mesh sizes of ~11N and ~15N, we concluded that mesh convergence has been reached with size ~11N.

To study the properties of the system at low Reynolds numbers, the input velocity v was lowered. The new nominal operating point of this system is (u = 0, $v = 3\times10^{-4}$ m/s) which corresponds to Re = 21. An 892-node mesh was constructed with higher mesh density in the regions of primary interest in order to increase the model accuracy. To validate the nonlinear model, a series of mesh refinements were carried out again to obtain a converged solution. ADINA® simulation runs were performed for N = 892 nodes, ~2N, ~4N, ~8N, and ~10N. The nature of the solution does not change as the number of the mesh nodes is increased indicating mesh convergence. The velocity profiles were computed for locations y = 1m, 2m, 3m, and 4m measured from the step and are shown in Figure 6 for the case Re = 21. In the region of interest, where the reattachment point forms (1m < y < 2m and 0m < z < 0.5m), the 892-node point mesh solution is virtually identical to the higher order mesh solutions. To ensure mesh independence in the region of interest (the location of the reattachment point), the mesh in that area had higher resolution. In the upper portion of the flow the mesh was quite coarse, especially at N mesh points, which resulted in a solution that was not very mesh independent. The results showed that such errors do not affect the solution in the region of interest. The open-loop disturbance response of the system is shown in Figure 7.

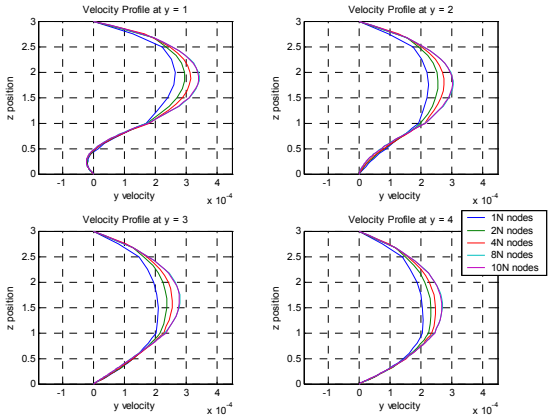

Figure 6. Nonlinear model validation: Velocity profiles at y = 1m, 2m, 3m, and 4m (Re = 21).

IV. Generation of Linear Models

We define the system state vector as x = $[v_y^t, v_z^T]^T$, where v_y is the vector of fluid velocity in the y-direction as measured at each node excepting the nodes embedded in the walls and v_z is the z-velocity vector. Notice that the pressure state variables were not included since pressure does not affect the velocity state variables (incompressible fluid). The system

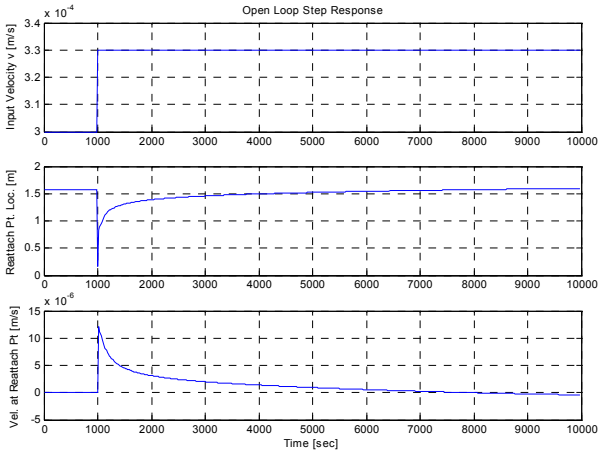

Figure 7. Open-loop step response (a) input disturbance signal (top plot), (b) reattachment point location (middle plot), and (c) velocity at the nominal reattachment point (bottom plot).

input vector is defined as u = $[v, u]^T$. The linear system output is the velocity vector v_y, which can in turn be used to calculate the flow reattachment point (through a nonlinear relationship).

In order to build a discrete nonlinear model of the system, first the sample period was chosen to be much less than the Courant number of this system [19]. Since the smallest nodal separation was approximately 0.1m in the y-direction and the largest velocity in this direction was approximately 1.0m/sec, dt = 0.01sec was chosen to ensure numerical stability A high-order linear model was obtained by numerical evaluation about the equilibrium (steady-state) solution $\mathbf{x_0}$, $\mathbf{u_0}$. By defining the state and input vectors as perturbations from the equilibrium (steady-state) solution, the linear discrete model can be written in standard form:

$$\mathbf{x}_{k+1} = \mathbf{A}\mathbf{x}_k + \mathbf{B}\mathbf{u}_k$$
$$y_k = v_y = \mathbf{C}\mathbf{x}_k = [\mathbf{I} \quad \mathbf{0}]\mathbf{x}_k \qquad (1)$$

To validate the linear models, a Pseudo-Random Binary Sequence (PRBS) [5] was selected to excite both the linear and nonlinear models. The outputs of the two models were compared at many nodes. Figure 8 shows a typical comparison plot. From the results we concluded that the high-order linear and the nonlinear models were consistent. Figure 9 shows the pole locations inside the unit circle for the high Reynolds number case. For this case the discrete time sampling period is T_s = 0.01 sec. The locations of the discrete poles range from 0.9754 to 0 and the damping coefficients range from ζ = 0.692 to unity. The linear system is non-minimum phase and has a transmission zero (not shown in Figure 9) on the real axis just outside the unit circle. Figure 10 shows the pole locations for Re = 21 case. The locations of the discrete poles range from 0.9964 to 6.1258e-7 and the damping coefficients range from ζ = 0.747 to unity. The system is minimum phase for this case.

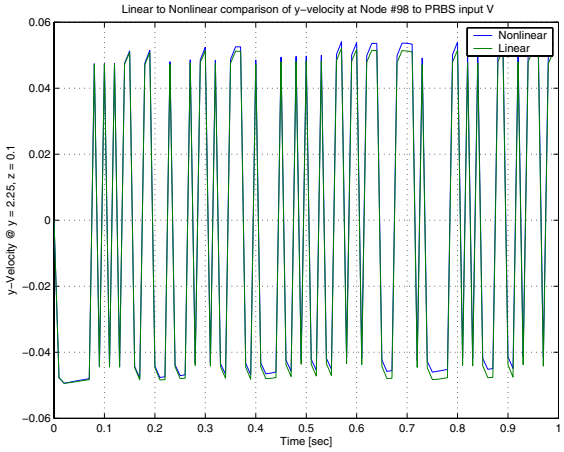

Figure 8. Comparison of the linear and nonlinear model responses at state variable 98 for PRBS excitation in *v* (for Re = 6.97 × 10^4).

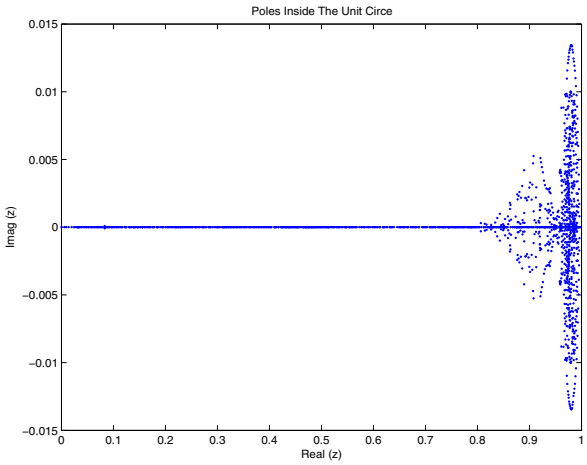

Figure 9. System poles inside the unit circle (Re = 6.97×10^4).

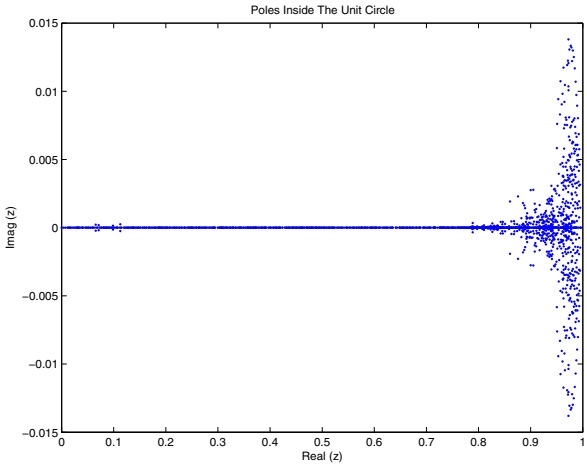

Figure 10. System poles inside the unit circle (Re = 21).

V. Plant Model Order Reduction

Two methods were used for model order reduction: balanced truncation and system identification from simulation data. As a means of evaluating the potential for model-order reduction, the controllability and observability Gramians (**P**, **Q** respectively) were computed [17]-[18]:

$$\mathbf{APA}^{\mathrm{T}} - \mathbf{P} + \mathbf{BB}^{\mathrm{T}} = 0 \qquad (2)$$
$$\mathbf{A}^{\mathrm{T}}\mathbf{QA} - \mathbf{Q} + \mathbf{C}^{\mathrm{T}}\mathbf{C} = 0$$

The Hankel singular values of the system were computed and the normalized values are plotted in Figure 11.

$$\sigma_i = \lambda_i^{1/2}(\mathbf{PQ}) \qquad (3)$$

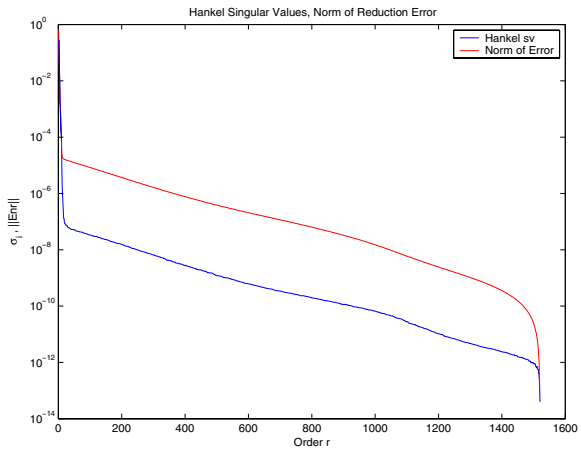

Figure 11. Hankel singular values and norm of reduction error (Re = 6.97 × 10^4).

Assume that an r^{th} order reduced order model was selected from the balanced system,

$$G_r(z) = \mathbf{C}_1(z\mathbf{I} - \mathbf{A}_{11})^{-1}\mathbf{B}_1 \qquad (4)$$

then the reduction error is

$$E_{n-r}(z) = G(z) - G_r(z) \qquad (5)$$

where

$$G(z) = \mathbf{C}(z\mathbf{I} - \mathbf{A})^{-1}\mathbf{B} \qquad (6)$$

and for any r, $1 \le r \le n-1$,

$$\| E_{n-r}(z) \|_\infty \le 2 \sum_{i=r+1}^{n} \sigma_i \qquad (7)$$

(and strict inequality holds if $\sigma_i \neq \sigma_{i+1}$ for any i, $r \le i \le n-1$). The reduction error was computed and is also displayed in Figure 11. The Hankel singular values were also computed for the low Reynolds number case (Re = 21), and show a very similar trend. In both cases, amazingly (!) the results suggest a fourth-order reduced plant model. Reduced order plant models were also derived using linear system identification with simulation data. In our case, we excited the high-order linear model with persistently exciting input signal consisting of a combination of steps with a Pseudo-Random-Binary-Sequence (PRBS). We used a prediction error method to identify the dynamics [16]. An autoregressive with an external input (ARX) model structure was chosen and standard routines from the MATLAB® System Identification toolbox were used. Separate models were identified for the transfer functions

from the inputs v and u to the output velocities as recorded along the bottom wall of the modified backward-facing step. All of these transfer functions could be described by either a 3rd or 4th order dynamic system.

The measurements of the flow velocity directly above the lower wall were used to determine the reattachment point: the point where the velocity is zero. This location was determined by interpolation between the two nodes where the velocity changed sign.

We also identified a local transfer function that directly describes the dynamics from v and u to the reattachment point. Again, 3rd and 4th order models were sufficient to very accurately predict the local flow behavior. These system identification results corroborated the results obtained earlier from balanced truncation studies. Hence, we decided to use a 4th order reduced order model for the feedback regulator designs discussed in the next section.

VI. Feedback Control System Design

Our goal is to design a robust controller for regulation and tracking. We have used the "error space" approach for designing robust feedback regulators [5]. A block diagram of the closed-loop system is shown in Figure 12.

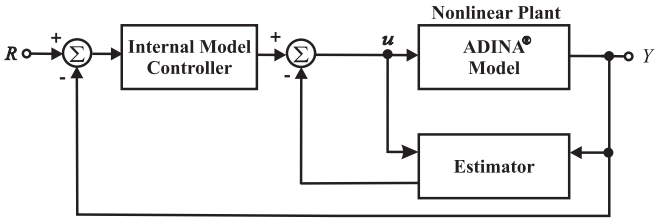

Figure 12. Control structure.

A. Disturbance Rejection

A double integral sixth order LQG controller was designed using the error space approach for the case Re = 6.97 × 10^4. The double integral control was required because of the presence of the non-minimum phase plant transmission zero mentioned before. The controller was tested on the full order (1520 state variable) plant model derived in Section IV. A comparison of the response of the linear closed-loop model and the nonlinear ADINA® closed-loop model is shown in Figure 13. It is seen that the linear and nonlinear closed-loop simulations are in good agreement. There is a long "tail" on the response due to the presence of slow poles. This suggests the potential need for time-optimal control.

The design was repeated for the 1568 state variable plant model (Re = 21) but for a single integral internal model control due to the fact that the system is minimum-phase. A 5th order internal model controller was designed. The controller was tested on the full order (1568 state variable) plant model. Figure 14 shows the disturbance rejection property of the nonlinear closed-loop ADINA® model with the disturbance injected at t = 10,000 sec. The plot also shows the open-loop step disturbance response for comparison purposes. The closed-loop system rejects the disturbance rapidly.

B. Tracking Control

Reattachment point tracking control was achieved using feedback control for both the high and low Reynolds number cases. The control was used to adjust the input velocity of the u stream to track the desired location. The regulator controllers described above were used to provide feedback control to reduce the velocity at the commanded reattachment point to zero. Figure 15 shows the tracking response of the nonlinear closed-loop system for various reattachment point step commands for the low Reynolds number case (Re = 21). It is seen that tracking of the reattachment points is achieved rapidly by the feedback controller using smooth control signals. For this case, the reattachment point was commanded to follow an upward

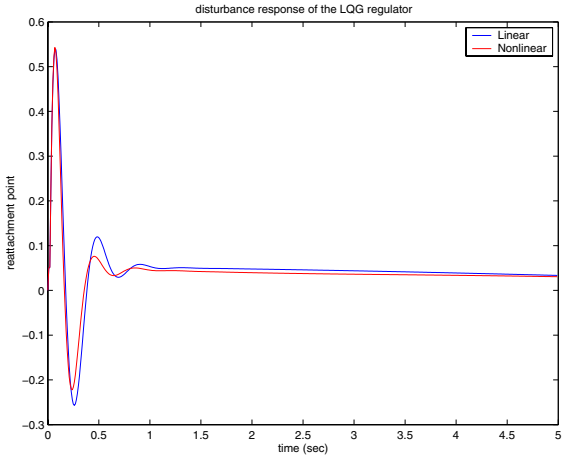

Figure 13. Comparison of the nonlinear and linear regulator closed-loop response for a step disturbance (Re = 6.97×10^4).

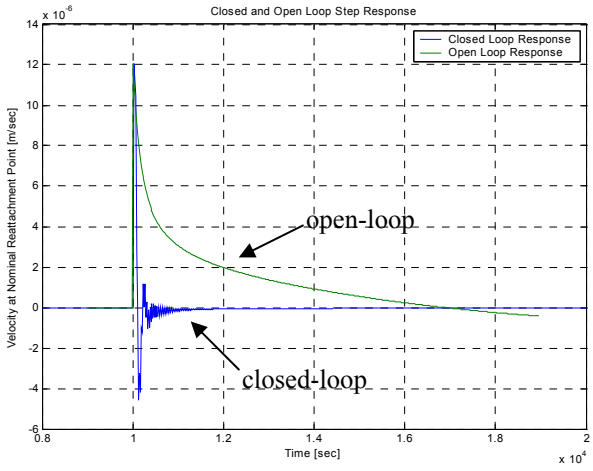

Figure 14. Nonlinear regulator closed-loop response with a constant disturbance injected at t = 10,000 sec (Re = 21), using the LQG controller, and comparison with open-loop disturbance response.

step (i.e., move the reattachment point 0.1 m to the right), a downward step (i.e., move the reattachment point to the left by 0.2m), and return to the nominal position (i.e., the nominal reattachment point position at y = 1.57m). As can be seen from Figure 15, the controller quickly follows these commands and moves the reattachment point to its new commanded locations. A MATLAB® simulation was developed to visualize the closed-loop nonlinear response as shown in Figure 16 where the arrow shows the location of the reattachment point.

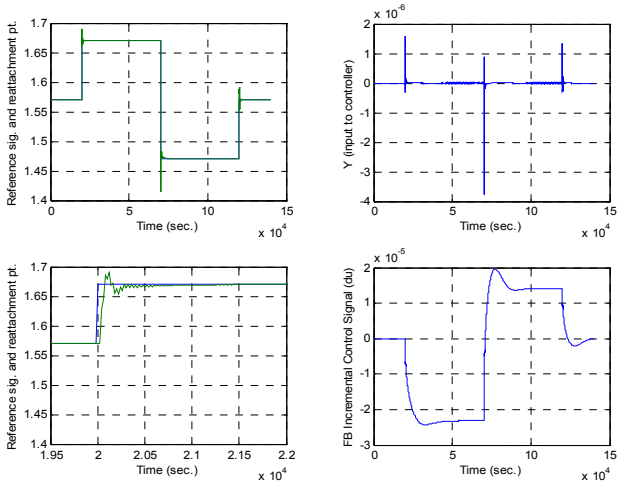

Figure 15. Tracking response of the nonlinear closed-loop system for reattachment point for various step commands (Re = 21).

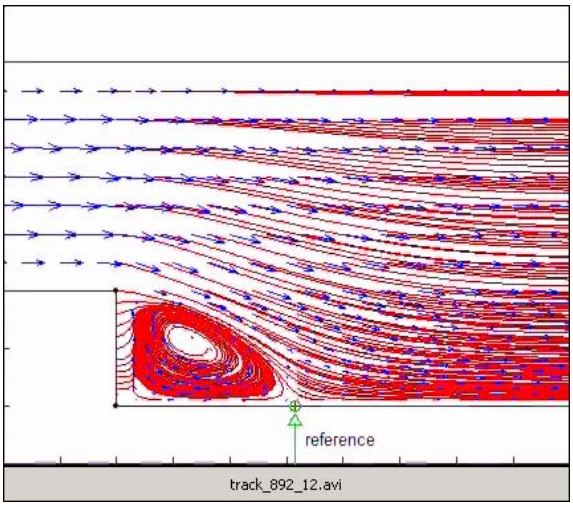

Figure 16. A snapshot of a MATLAB® movie of the reattachment point tracking response (Re = 21).

VII. CONCLUSION

An effective approach for model reduction for active flow control design was developed. We evaluated various reduction algorithms on high dimensional models for flow over backward-facing step models. The feasibility of the methodology was demonstrated by application of separation control for the 2D backward-facing step problem. Models were developed for high and low Reynolds numbers. Methods of reducing a high order plant model followed by a low-order controller design were investigated. Plant model order reduction using balanced truncation as well as system identification proved to be very effective yielding a reduction of model order from a 1520-1568 full order to a 4th order reduced order model. Disturbance rejection and tracking of the reattachment point was achieved using LQG controllers.

VIII. ACKNOWLEDGEMENT

The contributions of Professor Bassam Bamieh of UCSB and Dr. Sarbajit Ghosal of SC Solutions, Inc. are gratefully acknowledged. The authors would also like to thank Dr. James Myatt, Capt. Ian S. Bautista, Mr. Russell Camphouse, and Dr. J. Evers of USAF for their suggestions and feedback.

REFERENCES

[1] M. Gad-el-Hak, *Flow Control: Passive, Active, and Reactive Flow Management,* Cambridge University Press, 2000.

[2] T. R. Bewley, H. Choi, R. Temam, and P. Moin, "Optimal feedback control of turbulent channel flow," *Annual Research Briefs*, Center for Turbulence Research, Stanford Univ./NASA Ames, 1993.

[3] H. Choi, M. Hinze, and K. Kunisch, "Instantaneous Control of Backward-Facing Step Flows," *Applied Numerical Mathematics*, 31, pp. 133-158, 1999.

[4] P. Moin and T. Bewley, "Feedback Control of Turbulence," *Applied Mechanics Reviews*, Vol. 47, No. 6, Part 2, pages S3-S13; June 1994.

[5] G. F. Franklin, J. D. Powell, A. Emami-Naeini, *Feedback Control of Dynamic Systems*, 4th Ed., Prentice-Hall, 2002.

[6] B. Bamieh and M. Dahleh, "Energy amplification in channel flows with stochastic excitation," *Physics of Fluids*, 13(11): 3258--3269, 2001.

[7] M. Jovanovic and B. Bamieh, "Lyapunov-based distributed control of systems on lattices," submitted to *IEEE Trans. Automatic Control*, 2002.

[8] M. Jovanovic and B. Bamieh, "Modeling flow statistics using the linearized Navier-Stokes equations," *Proc. 40th IEEE Conference on Decision and Control*, Orlando, FL, 2001.

[9] M. Jovanovic and B. Bamieh, "The spatio-temporal impulse response of the linearized Navier-Stokes equations," *Proc. American Control Conference*, 2001.

[10] R. Camphouse and J. Myatt, "Feedback Control for a Two-Dimensional Burger's Equation System Model," *2nd AIAA Flow Control Conference*, AIAA-2004-2411, June 2004.

[11] J. Kim, S. J. Kline, and J. P. Johnston, "Investigation of a Reattaching Turbulent Shear Layer: Flow over a Backward-facing Step," *J. of Fluid Engr*., Vol. 102, 302-308, Vol. 102, Sept. 1980.

[12] J. J. Kim, "Investigation of Separation and Reattachment of a Turbulent Shear Layer: Flow Over a Backward-Facing Step," Ph.D. Dissertation, Stanford University, April 1978.

[13] H. Le, P. Moin, and J. Kim, "Direct Numerical Simulation of Turbulent Flow Over a Backward-Facing Step," *J. Fluid Mech*., vol. 330, pp. 349-374, 1997.

[14] V. Michelassi, et al.., "Prediction of the backflow and recovery regions in the backward facing step at various Reynolds numbers," Center for Turbulence Research, Stanford University, Proc. Summer Program 1996.

[15] B. Bamieh and M. Dahleh, "Energy amplification in channel flows with stochastic excitation," *Physics of Fluids*, 13(11), 2001.

[16] Ljung, *System Identification, Theory for the User*. Prentice-Hall, Englewood Cliffs, NJ, 1987.

[17] U. M. Al-Saggaf and G. F. Franklin, "On Model Reduction," in *Proc. 25th IEEE Conf. Dec. Contr*., pp. 1064-1069, December 1986.

[18] U. M. Al-Saggaf, "On Model Reduction and Control of Discrete Time Systems," Ph.D. Dissertation, Stanford University, June 1986.

[19] J. H. Ferziger and M. Peric, *Computational Methods for Fluid Dynamics*, Springer, 1997.